

Suppression of Shot-Noise in Quantum Cavities: Chaos vs. Disorder

Ph. Jacquod* and Robert S. Whitney*

**Département de Physique Théorique, Université de Genève, CH-1211 Genève 4, Switzerland*

Abstract. We investigate the behavior of the shot-noise power through quantum mechanical cavities in the semiclassical limit of small electronic wavelength. In the absence of impurity scattering, the Fano factor F , giving the noise to current ratio, was previously found to disappear as more and more classical, hence deterministic and noiseless transmission channels open up. We investigate the behavior of F as diffractive impurities are added inside the cavity. We find that F recovers its universal value provided (i) impurities cover the full cavity so that only a set of zero measure of classical trajectories may avoid them, and (ii) the impurity scattering rate exceeds the inverse dwell time through the cavity. If condition (i) is not satisfied, F saturates below its universal value, even in the limit of strong scattering. Our results corroborate the validity of the two-phase fluid model according to which the electronic flow splits into two well separated components, a classical deterministic fluid and a stochastic quantum-mechanical fluid. Only the latter carries shot-noise.

Time-resolved transport measurements through quantum mechanical systems invariably observe current fluctuations, even in the (experimentally unrealistic) situation of a noiseless measurement apparatus and at zero temperature. This intrinsically quantal noise is usually referred to as shot-noise. It results from the quantization of charge together with the statistical nature of quantum mechanical transport [1]. As but one of the consequences of the quantum-classical correspondence at large quantum numbers, it has been predicted that, shot-noise through a chaotic ballistic cavity disappears as the system becomes more and more classical, i.e. when the ratio of the electronic Fermi wavelength to the linear cavity size vanishes $\lambda_F/L \rightarrow 0$ [2]. The purpose of this article is to discuss when and how shot-noise starts to be reduced by an emergent classical, deterministic behavior.

Recent technological advances have made it possible to make electronic systems small and clean enough that the resulting electronic mean free path is larger than the size of the confining potential defining the device [3]. The electronic motion in these quantum dots is thus ballistic, and provided that their wavelength is short enough, the electrons have a dynamics strongly related to the dynamics that a classical particle would have. When this classical dynamics is chaotic, that is, when the shape of the dot differs significantly from a circle or an ellipse, the transport properties are usually universal and well-captured by the Random Matrix Theory (RMT) of transport [4]. The starting point of RMT is the scattering approach [5], which relates transport properties to the system's scattering matrix

$$\mathcal{S} = \begin{pmatrix} \mathbf{r} & \mathbf{t}' \\ \mathbf{t} & \mathbf{r}' \end{pmatrix}. \quad (1)$$

Here we consider a symmetric two terminal geometry (the cavity is connected to two external leads with equal number N of propagating channels) for which \mathcal{S} is a 2-block by 2-block matrix, written in terms of $N \times N$ transmission (\mathbf{t} and \mathbf{t}') and reflection (\mathbf{r} and \mathbf{r}') matrices. From \mathcal{S} , the system's conductance is given by $g = \text{Tr}(\mathbf{t}^\dagger \mathbf{t}) = \sum_n T_n$ (g is expressed in units of e^2/h and the T_n 's are the N eigenvalues of $\mathbf{T} = \mathbf{t}^\dagger \mathbf{t}$). RMT provides a statistical theory of transport where \mathcal{S} is assumed to be uniformly distributed over one of Dyson's circular ensemble of random matrices [6]. Transport properties can be calculated from this sole assumption. For instance, within RMT, and in the limit $N \gg 1$ the transmission eigenvalues have a probability distribution [4]

$$P_{\text{RMT}}(T) = \frac{1}{\pi} \frac{1}{\sqrt{T(1-T)}} \quad (2)$$

for any $T \in [0, 1]$. Note that classical particles would be either deterministically transmitted, $T = 1$ or reflected $T = 0$.

The distribution of transmission eigenvalues is all one needs to get fluctuations and higher moments of the current at low frequency. The zero-frequency shot-noise power in particular is given by $S = 2eV \sum_n T_n(1 - T_n)$ [1]. According to (2), S is suppressed below its Poissonian value of $S_p = 2e\langle I \rangle$ (V is the applied voltage and $\langle I \rangle$ the time-averaged current) by the Fano factor which reads

$$F = \frac{\sum_n T_n(1 - T_n)}{\sum_n T_n} \quad ; \quad F_{\text{RMT}} = \frac{1}{4}. \quad (3)$$

The RMT predictions (2) and (3) have been confirmed in various transport experiments and numerical simulations on open chaotic cavities [1, 4].

In closed chaotic systems, the semiclassical limit $\lambda_F/L \equiv \hbar_{\text{eff}} \rightarrow 0$ usually results in a better and better agreement with the Hamiltonian RMT of spectral fluctuations [7]. One may thus expect that the same applies to transport in open systems. That is not so, as illustrated in Fig. 1. The numerical data presented there (see also Ref. [8]) show that instead of the RMT prediction of Eq. (2), the transmission eigenvalues appear to be distributed according to

$$P_\alpha(T) = \alpha P_{\text{RMT}}(T) + \frac{1-\alpha}{2} [\delta(T) + \delta(1-T)], \quad (4)$$

with an increasingly deterministic behavior $\alpha \rightarrow 0$ as $\hbar_{\text{eff}} \rightarrow 0$ (all classical parameters being fixed). The presence of δ -peaks at $T = 0$ and $T = 1$ in $P_\alpha(T)$ becomes evident once the integrated distribution $I(T) = \int_0^T P(T') dT'$ is plotted. One has

$$I_\alpha(T) = \frac{2\alpha}{\pi} \sin^{-1} \sqrt{T} + \frac{1-\alpha}{2} (1 + \delta_{1,T}), \quad (5)$$

so that $I_\alpha(0) = (1-\alpha)/2$ vanishes only for $\alpha = 1$. It turns out that the parameter α is well approximated by $\alpha \approx \exp(-\tau_e/\tau_d)$, in term of the new time scale $\tau_e = -\lambda^{-1} \ln[\hbar_{\text{eff}} \tau_d^2]$ and the average dwell time τ_d through the cavity [8]. In short, for a classically fixed configuration (i.e. considering an ensemble of systems with fixed

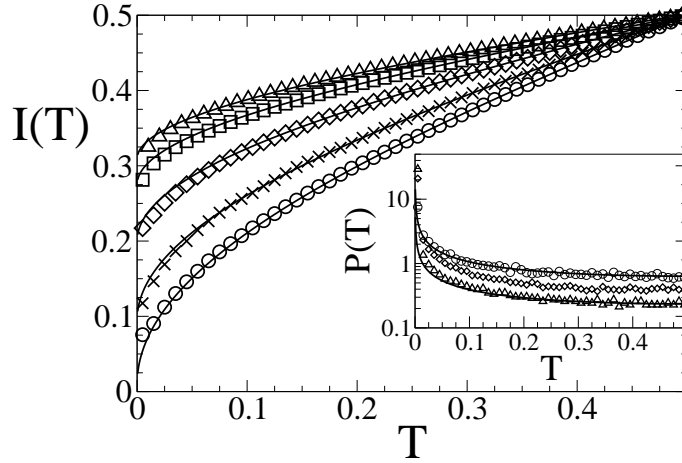


FIGURE 1. Integrated probability distribution $I(T)$ of transmission eigenvalues for $\tau_D = 25$, $\hbar_{\text{eff}}^{-1} = 2048$ and $\tau_E \simeq 0$ (circles; distribution calculated over 729 different samples); $\tau_D = 5$, $\hbar_{\text{eff}}^{-1} = 128$ and $\tau_E = 0.16$ (\times ; 1681 samples), $\hbar_{\text{eff}}^{-1} = 1024$ and $\tau_E = 1.5$ (diamonds; 729 samples), $\hbar_{\text{eff}}^{-1} = 8192$ $\tau_E = 2.8$ (squares; 16 samples), $\hbar_{\text{eff}}^{-1} = 65536$ and $\tau_E = 4.1$ (triangles; 2 samples). The solid curves give the distribution I_α of Eq. (5), with $\alpha \approx 0.98, 0.81, 0.6, 0.45$, and 0.385 (from bottom to top). Inset: Probability distribution $P(T)$ of transmission eigenvalues for the same set of parameters as in the main panel (squares and \times have been removed for better visibility). The solid curves give the universal distribution P_{RMT} of Eq. (2) and that of Eq. (4), with $\alpha = 0.39$ (from top to bottom). Note that $P(T)$ is symmetric around $T = 0.5$.

λ and τ_d), the fraction $(1 - \alpha)/2$ of deterministic transmission eigenvalues $T = 0, 1$ increases as one goes deeper and deeper into the semiclassical limit, $\hbar_{\text{eff}} \rightarrow 0$. The rate of the crossover is set by a partially quantum, partially classical time scale, the *Ehrenfest time* τ_e [9]. Compared to closed systems, the emergence of a finite τ_e has more profound an impact on transport properties once it becomes comparable to the dwell time $\tau_d \propto (N\hbar_{\text{eff}})^{-1}$.

Inserting (4) into (3) with the numerically extracted value $\alpha \approx \exp(-\tau_e/\tau_d)$, one directly recovers $F \propto \exp[-\tau_e/\tau_d]$, in agreement with the analytical prediction of Refs. [10, 11], the experimental results of Ref. [12] and the numerical data of Ref. [13]. They can be qualitatively understood by first realizing that complex quantum systems split into the two classes of quantum chaotic and quantum disordered systems [14]. Ballistic cavities in particular belong to the first class, for which electronic wavepackets are carried along very few classical paths until the time τ_e after which they have a finite probability to be found on trajectories that their center of mass would not follow classically. This dynamical diffraction process restores quantum mechanical stochasticity for larger times, however it does not affect short trajectories with $\tau < \tau_e$. Thus, in quantum chaotic systems, two classes of classical trajectories emerge, depending on their dwell time through the cavity. Short trajectories with $\tau < \tau_e$ are able to carry an electronic wavepacket deterministically through the cavity (i.e. with transmission probability $T = 0$ or 1). If the electronic wavepacket sits on longer trajectories with $\tau > \tau_e$ on the other hand, diffraction splits it into pieces before its exit, and quantum mechanical stochasticity (with $T \in]0, 1[$) prevails. The fraction of scattering trajectories in the

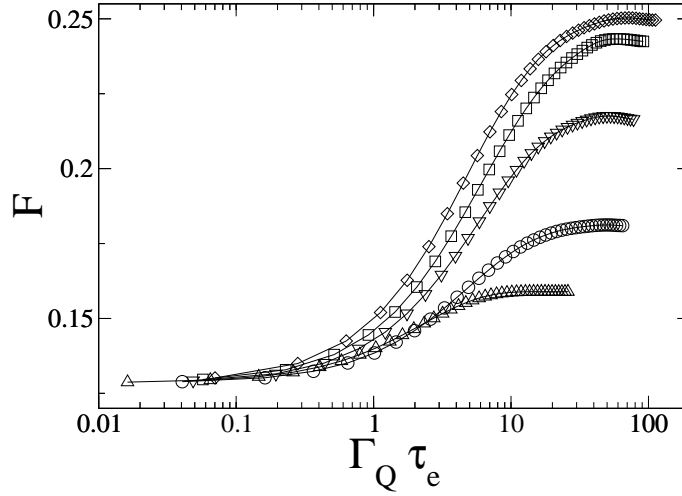


FIGURE 2. Crossover from quantum chaotic behavior (left) to quantum disordered behavior (right) of the Fano factor F as a function of $\Gamma_Q \tau_e$. Each set of data corresponds to an average over four different samples with $\hbar_{\text{eff}}^{-1} = 8192$, $K = 7.65$, $\tau_D = 5$ and $\xi = 1250$ (upward triangles), 2500 (circles), 3750 (downward triangles), 5000 (squares) and 7500 (diamonds).

stochastic subset is obtained via the dwell time distribution $\rho(\tau)$ by

$$\alpha \equiv \int_{\tau_e}^{\infty} \rho(\tau) d\tau. \quad (6)$$

In a chaotic system one has $\rho(\tau) = \tau_d^{-1} \exp[-\tau/\tau_d]$, hence the fraction of stochastically transmitted channels gives $\alpha \approx \exp[-\tau_e/\tau_d]$ for the weight α of Eq. (4), in agreement with the numerics shown in Fig. 1. This is the essence of the *two-phase-fluid model* [8], originally proposed in Ref. [11] and given a microscopic foundation in Ref. [16]

Fig. 1 provides us with a direct evidence for the validity of the two-phase fluid. Other evidences of this kind have been found in investigations of the excitation spectrum of Andreev billiards, i.e. ballistic cavities in contact with a superconductor [15]. In a previous work [16], we used an approach based on a semiclassical expansion for the Green's function in term of a sum over classical trajectories. Together with the construction of a quantum-mechanical phase-space basis, this allowed us to import classical concepts such as Liouville conservation and determinism into quantum mechanics, thereby providing with a microscopic foundation for the two-phase fluid model [17]. Our purpose in the reminder of this article is to check numerically the model by investigating its quantum chaos – quantum disorder crossover.

To this end, we use the open kicked rotator model and follow the procedure described e.g. in Ref. [13]. So far, the model has been implemented only in its quantum chaotic version. Here we add a diffraction term to it so that its Floquet (time-evolution) operator has matrix elements

$$U_{m,m'} = \hbar_{\text{eff}}^{1/2} e^{-(iK/4\pi\hbar_{\text{eff}})[\cos(2\pi m\hbar_{\text{eff}}) + \cos(2\pi m'\hbar_{\text{eff}})]} e^{-(i/4\pi\hbar_{\text{eff}})[\eta(m) + \eta(m')]} \\ \times \sum_l e^{2\pi i l(m-m')\hbar_{\text{eff}}} e^{-(\pi i \hbar_{\text{eff}}/2)l^2}, \quad (7)$$

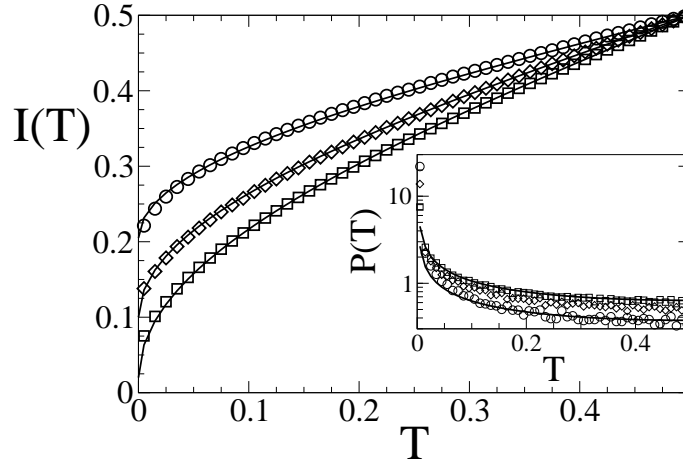


FIGURE 3. Integrated probability distribution $I(T)$ of transmission eigenvalues for the open kicked rotator model with diffractive disorder of Eq. (7). The data have been obtained from 16 different samples with parameters $\hbar_{\text{eff}}^{-1} = 8192$, $K = 7.65$, $\tau_D = 5$ and $u = 0.4$, with $\xi = 0$ (circles), 2500 (diamonds), and 7500 (squares). The solid curves give the distribution I_α of Eq. (5), with $\alpha \approx 0.99, 0.76$, and 0.52 from bottom to top. Inset: Probability distribution $P(T)$ of transmission eigenvalues for the same set of parameters as in the main panel. The solid curves give the universal distribution P_{RMT} of Eq. (2) and that of Eq. (4), with $\alpha = 0.59$ respectively.

with a randomly distributed function $\langle \eta(m)\eta(m') \rangle = u^2 \delta_{m,m'} \Theta(|m - m_0| - \xi/2)$. Such a point-like diffractive impurity potential corresponds to the extreme quantum disorder limit. The length scale ξ allows to cover all or only a part of the system, and u sets the strength of the impurity scattering. We extracted the scattering rate Γ_Q from the width of the Local Spectral Density of States (LDOS) induced by $\eta(m)$ for the closed kicked rotator. As is commonly the case [18], we found that the LDOS has a Lorentzian shape with a width $\Gamma_Q \approx 0.016 u^2 \sqrt{\xi} / \hbar_{\text{eff}}$ in a wide range of parameter. One expects that, as Γ_Q becomes comparable to the Ehrenfest time, quantum diffraction effects start to eat away the determinism of short trajectories.

We first show in Fig. 2 the behavior of the Fano factor as the diffractive scattering rate is cranked up, all other parameter being fixed. For $\Gamma_Q = 0$, $F < 0.25$ lies below its universal value, indicating a finite τ_e , thus a finite fraction of non-diffractive scattering orbits. This fraction gets reduced once Γ_Q increases, and accordingly $\partial F / \partial \Gamma_Q > 0$. The most striking feature of Fig. 2, however, is that as long as the diffractive disorder does not cover the whole system volume, i.e. for $\xi < \hbar_{\text{eff}}^{-1} (1 - \tau_d^{-1})$, F saturates below its universal value, even in the limit $\Gamma_Q \tau_e \rightarrow \infty$. This reflects the fact that some short trajectories are able to avoid the diffractive potential and thus remain deterministic. The existence of two separated phase-space fluids allows only that part of the deterministic fluid which directly scatters off the impurities to become stochastic. It is not clear from our numerics if, for $\xi > \hbar_{\text{eff}}^{-1} (1 - \tau_d^{-1})$, one has an exponential or a power-law behavior of the Fano factor as predicted in Ref. [12, 19]. More detailed investigations are necessary to draw definite conclusions.

We finally show on Fig. 3 the behavior of the distribution of transmission eigenvalues in the saturated regime $\Gamma_Q \tau_e \gg 1$. Clearly, the distribution and integrated distribution

follow Eqs. (4) and (5). In contrast to the quantum chaotic case, we qualitatively found a dependence $\alpha \propto \exp[-\tau_e/\tau_d] \xi \hbar_{\text{eff}}/(1 - \tau_d^{-1})$, again reflecting a reduction of that part of the deterministic component which directly touches the diffractive potential.

All these findings support the two-phase fluid hypothesis, that is, the splitting of the cavity into a stochastic and a deterministic cavity. The latter being noiseless, shot-noise is suppressed by a factor reflecting its phase-space measure relative to the total phase-space. This measure is reduced by the presence of diffractive disorder, however, only homogeneously spread impurities are able to diffract all trajectories, thus only in this case does one recover universality at large diffractive scattering rate. This complement recent investigations of shot-noise with homogeneously spread diffractive disorder in regular cavities [20].

This work has been supported by the Swiss National Science Foundation.

REFERENCES

1. For a review on shot-noise, see : Ya.M. Blanter and M. Büttiker, Phys. Rep. **336**, 1 (2000).
2. C.W.J. Beenakker and H. van Houten, Phys. Rev. B **43**, R12066 (1991).
3. L.P. Kouwenhoven, C.M. Marcus, P.L. McEuen, S. Tarucha, R.M. Westervelt, and N.S. Wingreen, *Electron Transport in Quantum Dots*, Nato ASI conference proceedings, L.P. Kouwenhoven, G. Schön, and L.L. Sohn Eds. (Kluwer, Dordrecht, 1997); Y. Alhassid, Rev. Mod. Phys. **72**, 895 (2000).
4. C.W.J. Beenakker, Rev. Mod. Phys. **69**, 731 (1997).
5. R. Landauer, Phil. Mag. **21**, 863 (1970); M. Büttiker, Phys. Rev. Lett. **57**, 1761 (1986).
6. M. L. Mehta, *Random Matrices* (academic, New York, 1991).
7. F. Haake, *Quantum Signatures of Chaos*, (Springer, Berlin, 2000).
8. Ph. Jacquod, and E.V. Sukhorukov, Phys. Rev Lett. **92** 116801 (2004).
9. G.M. Zaslavsky, Phys. Rep. **80**, 157 (1981); M.G. Vavilov and A.I. Larkin, Phys. Rev. B **67**, 115335 (2003).
10. O. Agam, I. Aleiner and A. Larkin, Phys. Rev. Lett. **85**, 3153 (2000).
11. P.G. Silvestrov, M.C. Goorden, and C.W.J. Beenakker, Phys. Rev. B **67**, 241301(R) (2003).
12. S. Oberholzer, E.V. Sukhorukov, and C. Schönenberger, Nature **415**, 765 (2002).
13. J. Tworzydło, A. Tajic, H. Schomerus, and C.W.J. Beenakker, Phys. Rev. B **68**, 115313 (2003).
14. I.L. Aleiner and A.I. Larkin, Phys. Rev. B **54**, 14423 (1996).
15. M.C. Goorden, Ph. Jacquod, and C.W.J. Beenakker, cond-mat/0505206.
16. R.S. Whitney, and Ph. Jacquod, Phys. Rev. Lett. **94**, 116801 (2005).
17. We note that the prediction of the two-phase fluid model that coherent effects such as weak localization do not depend on τ_e have recently been criticized; see S. Rahav and P.W. Brouwer, cond-mat/0505250. It is not our purpose here to discuss this point in detail. Instead we will present elsewhere a semiclassical calculation of weak localization contradicting the results of Rahav and Brouwer and supporting the survival of the weak localization corrections to conductance at their universal value independently of τ_e ; Ph. Jacquod and R.S. Whitney, in preparation (2005).
18. Ph. Jacquod and D.L. Shepelyansky, Phys. Rev. Lett. **75**, 3501 (1995).
19. E.V. Sukhorukhov and O.M. Bulashenko, Phys. Rev. Lett. **94**, 116803 (2005).
20. F. Aignier, S. Rotter, and J. Burgdörfer, cond-mat/0502417.